Bone 121 (2019) 29–41

Contents lists available at ScienceDirect

Bone

journal homepage: www.elsevier.com/locate/bone

Full Length Article

Constitutive activation of the alternative NF-κB pathway disturbs endochondral ossification

Chihiro Nakatomi[a], Mitsushiro Nakatomi[b], Takuma Matsubara[a], Toshihisa Komori[c], Takahiro Doi-Inoue[d], Naozumi Ishimaru[e], Falk Weih[f,1], Tsutomu Iwamoto[g], Miho Matsuda[h], Shoichiro Kokabu[a], Eijiro Jimi[a,h,i,*]

[a] Division of Molecular Signaling and Biochemistry, Kyushu Dental University, 2-6-1 Manazuru, Kokurakita-kux, Kitakyushu 803-8580, Japan
[b] Division of Anatomy, Department of Health Improvement, Kyushu Dental University, 2-6-1 Manazuru, Kokurakita-ku, Kitakyushu 803-8580, Japan
[c] Department of Cell Biology, Unit of Basic Medical Sciences, Nagasaki University Graduate School of Biomedical Sciences, 1-7-1 Sakamoto, Nagasaki 852-8588, Japan
[d] Hanzomon Hospital, 1-10-5 Kojimachi, Chiyoda-ku, Tokyo 102-0083, Japan
[e] Department of Oral Molecular Pathology, Tokushima University Graduate School of Biomedical Sciences, 3-18-15 Kuramoto, Tokushima 770-8504, Japan
[f] Research Group Immunology, Leibniz-Institute on Aging – Fritz Lipmann Institute, Beutenbergstrasse 11, Jena 07745, Germany
[g] Department of Pediatric Dentistry, Tokushima University Graduate School of Biomedical Sciences, 3-18-15 Kuramoto, Tokushima 770-8504, Japan
[h] Laboratory of Molecular and Cellular Biochemistry, Kyushu University, 3-1-1 Maidashi, Higashi-ku, Fukuoka 812-8582, Japan
[i] Oral Health/Brain Health/Total Health Research Center, Faculty of Dental Science, Kyushu University, 3-1-1 Maidashi, Higashi-ku, Fukuoka 812-8582, Japan

ARTICLE INFO

Keywords:
Chondrocytes
Alternative NF-κB pathway
Endochondral ossification

ABSTRACT

Endochondral ossification is important for skeletal development. Recent findings indicate that the p65 (RelA) subunit, a main subunit of the classical nuclear factor-κB (NF-κB) pathway, plays essential roles in chondrocyte differentiation. Although several groups have reported that the alternative NF-κB pathway also regulates bone homeostasis, the role of the alternative NF-κB pathway in chondrocyte development is still unclear. Here, we analyzed the *in vivo* function of the alternative pathway on endochondral ossification using p100-deficient ($p100^{-/-}$) mice, which carry a homozygous deletion of the COOH-terminal ankyrin repeats of p100 but still express functional p52 protein. The alternative pathway was activated during the periarticular stage in wild-type mice. $p100^{-/-}$ mice exhibited dwarfism, and histological analysis of the growth plate revealed abnormal arrangement of chondrocyte columns and a narrowed hypertrophic zone. Consistent with these observations, the expression of hypertrophic chondrocyte markers, type X collagen (ColX) or matrix metalloproteinase 13, but not early chondrogenic markers, such as Col II or aggrecan, was suppressed in $p100^{-/-}$ mice. An *in vivo* BrdU tracing assay clearly demonstrated less proliferative activity in chondrocytes in $p100^{-/-}$ mice. These defects were partly rescued when the *RelB* gene was deleted in $p100^{-/-}$ mice. Taken together, the alternative NF-κB pathway may regulate chondrocyte proliferation and differentiation to maintain endochondral ossification.

1. Introduction

The ossification process is classified into intramembranous and endochondral ossification [1–3]. Appendicular skeletons, vertebrae, and the majority of other bones are generated by endochondral ossification. Endochondral ossification occurs with the condensation of mesenchymal cells. These mesenchymal cells differentiate into chondrocytes to secrete type II collagen (Col II) and aggrecan, which are chondrocyte-specific matrix proteins. After proliferation and matrix production, chondrocytes exit the cell cycle and swell to become hypertrophic chondrocytes. These cells begin to secrete type X collagen (Col X) instead of Col II. Hypertrophic chondrocytes mineralize the surrounding matrix and attract blood vessels. Osteoblasts, which intrude into the cartilage with blood vessels, comprise the primary spongiosa [1–3]. During the elongation of long bones, the secondary ossification center is formed at the epiphyseal area of the bone. The remaining cartilage between the primary and secondary ossification centers is called the growth plate. The growth plate consists of the resting, proliferative, prehypertrophic, and hypertrophic zones, and a series of chondrocyte differentiation processes is observed in these zones [1–3]. The process

* Corresponding author at: Oral Health/Brain Health/Total Health Research Center, Faculty of Dental Science, Kyushu University, 3-1-1 Maidashi, Higashi-ku, Fukuoka 812-8582, Japan.
E-mail address: ejimi@dent.kyushu-u.ac.jp (E. Jimi).
[1] Deceased.

https://doi.org/10.1016/j.bone.2019.01.002
Received 9 October 2018; Received in revised form 28 December 2018; Accepted 2 January 2019
Available online 03 January 2019
8756-3282/

of endochondral ossification is regulated by transcription factors at each stage, such as sex-determining region Y-type high-mobility group box protein (Sox9) [4–6] and runt-related transcription factor 2 (Runx2) [7,8].

Nuclear factor κB (NF-κB) is a critical transcription factor that regulates immune responses, inflammation, cell proliferation, and skeletal development [9,10]. The NF-κB family is composed of p65 (RelA), c-Rel, RelB, p50/p105 (NF-κB1), and p52/p100 (NF-κB2). Under unstimulated conditions, IκB proteins bind to NF-κB dimers to prevent nuclear translocation. The IκB protein family consists of IκBα, IκBβ, Bcl-3, IκBε, IκBγ, p100 (the precursor of p52), and p105 (the precursor of p50). NF-κB can be activated by two distinct pathways, the classical and alternative pathways; it then regulates gene expression during various biological processes. Activation of the classical NF-κB pathway is triggered by the phosphorylation and degradation of IκB protein followed by translocation of the p65/p50 dimer into the nucleus, inducing the expression of target genes. The alternative pathway is activated by ligands such as lymphotoxin β (LTβ), B-cell activating factor (BAFF), and receptor activator of NF-κB ligand (RANKL) [10,11]. Upon binding of these ligands to the cell surface receptors, NF-κB inducing kinase (NIK) is activated to phosphorylate the IκB kinase (IKK) complex. Then, the activated IKK complex phosphorylates the p100 protein of the p100/RelB dimer, causing p100 to be processed to p52. This p52/RelB dimer translocates into the nucleus to induce target gene expression [10,11].

Several studies have reported that the NF-κB transcription family is involved in endochondral ossification and limb outgrowth. In the chick embryo, NF-κB genes are expressed in the progress zone of the limb bud [12], and IKKα deficient mice exhibit abnormal limb development [13,14]. Furthermore, the role of the classical NF-κB pathway in chondrocyte differentiation has been investigated in detail. NF-κB p65 is expressed in the growth plate and facilitates longitudinal bone growth by inducing chondrocyte proliferation and differentiation and by preventing apoptosis [15]. NF-κB expressed in growth plate chondrocytes mediates the promoting effects of growth hormone (GH) and insulin-like growth factor (IGF)-1 on longitudinal bone growth and growth plate chondrogenesis [16]. Recently, glycogen synthase kinase (GSK)-3α and GSK-3β have been shown to phosphorylate and activate RelA [17]; then, RelA induces the expression of Sox9 and a disintegrin and metalloproteinase with thrombospondin motifs 5 (Adamts5) in chondrocytes [18]. In addition, Pik3r1, an anti-apoptotic gene, has been identified as a direct transcriptional target gene of RelA in chondrocytes. RelA negatively regulates apoptosis in chondrocytes [19]. Constitutive activation of the classical NF-κB by IKKβ in osteoblasts and chondrocytes in mice exhibits abnormal skeletal development by suppression of chondrocyte maturation and osteoblast differentiation [20]. On the other hand, although the alternative NF-κB pathway regulates both osteoclastogenesis and osteoblastogenesis [21–26], the specific role of the alternative NF-κB pathway in chondrocytes has not been clarified.

In $p100^{-/-}$ mice, in which the ankyrin repeats in the C-terminus of NF-κB2 are homozygously deleted, the p100 protein cannot inhibit Rel/NF-κB activity, and DNA-binding activity of the p52/RelB complex is dramatically activated in various tissues [27]. As a result, $p100^{-/-}$ mice exhibit several disorders, such as gastric hyperplasia, atrophic spleen and thymus, and osteoporosis [23,27]. In this study, to elucidate the specific roles of the alternative NF-κB pathway in chondrocytes, we histologically and molecularly analyzed the cartilage phenotypes of $p100^{-/-}$ mice in detail.

2. Materials and methods

2.1. Mice

All animal experiments were reviewed and approved by the Kyushu Dental University Animal Care and Use Committee (Approved Number; 15-019). Generation of $p100^{-/-}$ mice and $RelB^{-/-}$ mice has been described previously [23,25]. $p100^{-/-}$ mice were mated with $RelB^{-/-}$ mice to generate $p100^{-/-}$;$RelB^{-/-}$ double knockout mice. All mouse lines were maintained on a C57BL/6J genetic background. Littermate wild-type (WT) mice were used as controls. At least three mice were collected for each analysis. Mice were maintained under standard laboratory conditions at 24 °C ± 2 °C and 50–60% humidity, and allowed free access to tap water and commercial standard rodent chow (CE-2) (Clea Japan inc., Tokyo, Japan). All mice were housed of Animal Research Center in the Kyushu Dental University with 12 h day-night cycle.

2.2. Tissue preparation

For Alcian Blue staining, postnatal day (P) 7 to P21 mice were perfused with physiological saline containing heparin, followed by a 4% paraformaldehyde (PFA) solution under deep anesthesia. Long bones were removed en bloc and immersed with the same fixative. Samples from embryos and newborn (P0) mice were fixed with immersion fixation only using 4% PFA. The obtained long bones were decalcified with Morse's solution. For *in situ* hybridization and immunohistochemistry, samples from embryonic day (E) 18.5 to P21 were fixed with Bouin's fixative. All the samples were dehydrated through an ethanol series, embedded in paraffin, and cut into 4-μm sections.

2.3. Alcian blue staining

Sections were deparaffinized, washed under running water, pretreated with 0.1 N HCl, stained with 1% Alcian Blue 8GX (Nacalai Tesque, Kyoto, Japan) solution for 90 min, posttreated with 0.1 N HCl, washed under running water, dehydrated, and mounted with Entellan® New (#107961; Merck Millipore Corp, Billerica, MA, USA).

2.4. Antibodies

The primary antibodies used in this study were anti-RelB (#sc-226; Santa Cruz Biotechnology, Santa Cruz, CA, USA), anti-IκBα (#sc-371; Santa Cruz), anti-HDAC1 (#sc-7872; Santa Cruz), anti-NF-κB2 (#4882S; Cell Signaling, Beverly, MA, USA, #GTX12226; GeneTex, Irvine, CA, USA), anti-phosphorylated NF-κB2 (#4810; Cell Signaling), anti-p65 (#SA171; Enzo Life Science, Farmingdale, NY, USA), anti-Col II (#ab21291; Abcam, Cambridge, MA, USA), anti-Col X (#2031501001; Quartett, Schichauweg, Berlin, Germany), anti-β-actin (#A5441; Sigma-Aldrich, St. Louis, MO, USA), and anti-5′-bromo-2′-deoxyuridine (BrdU) (#M0744; Dako, Denmark). Secondary antibodies were horseradish peroxidase (HRP)-conjugated anti-mouse IgG (#914; Sigma-Aldrich), HRP-conjugated anti-rabbit IgG (#4416; Sigma-Aldrich), Alexa Fluor 488-conjugated anti-rabbit IgG (#A-11008; Thermo Fisher Scientific, Waltham, MA, USA), and ProLong Gold antifade reagent with 4′,6-diamidino-2-phenylindole (DAPI) (#P36931, Thermo Fisher Scientific).

2.5. Immunohistochemistry

Sections were deparaffinized, immersed in phosphate buffered saline (PBS) containing 0.15% Triton X-100 for 30 min, rinsed with PBS three times, incubated with PBS containing 1% bovine serum albumin for 1 h for blocking, and incubated with primary antibodies overnight at 4 °C. The primary antibodies used in this study were anti-phosphorylated NF-κB2 (#4810; 1:100 dilution), anti-NF-κB2 (#GTX12226; 1:100 dilution) and anti-RelB (#sc-226; 1:100 dilution). The next day, the sections were rinsed with PBS three times, incubated with a secondary antibody (1:500 dilution) for 1 h at room temperature, rinsed with PBS five times, and mounted with ProLong Gold antifade reagent with DAPI.

2.6. Skeletal analysis

Skeletal staining of bone and cartilage was performed as described previously [28]. Briefly, after removing the skin and internal organs, the whole body was fixed with 95% ethanol, replaced with acetone, and stained with 0.1% Alcian Blue 8GX solution (Nacalai Tesque) for 3 h. After bleaching the color with 95% ethanol, samples were precleared with 1% KOH solution, stained with 0.03% Alizarin Red S solution (Wako Pure Chemical, Osaka, Japan), and cleared with 1% KOH solution. Samples were stored in 100% glycerol.

2.7. Western blotting

Proteins were extracted from primary chondrocytes derived from rib cartilage of newborn mice by digestion with 0.1% collagenase (Wako Pure Chemical). Cytosolic and nuclear extracts were prepared according to the method described by Dignam et al. [29]. Briefly, cells were lysed in Buffer A (10 mM HEPES pH 7.9, 10 mM KCl, and 0.1 mM EDTA) and 0.1% Nonidet P-40. Following centrifugation, the supernatant was collected as the cytosolic fraction. Precipitates were lysed in Buffer C (20 mM HEPES pH 7.9, 0.4 M NaCl, and 1 mM EDTA), and the supernatant was collected as the nuclear fraction after centrifugation. The protein content was measured by Pierce reagent according to the manufacturer's protocol. The lysates were resolved by 10% SDS-PAGE, transferred to Immobilon-P membranes (Millipore Corp.), and immunoblotted with individual antibodies. Then, the membranes were washed and incubated with horseradish peroxidase-conjugated secondary antibodies (Santa Cruz). The immunoreactive proteins were visualized using ECL (Amersham Pharmacia Biotech, Piscataway, NJ, USA) and were analyzed with a Luminescent Image Analyzer (Fujifilm, Tokyo, Japan).

2.8. In situ hybridization

Section *in situ* hybridization was performed as described previously [30]. The indian hedghog probe was kindly provided by Drs. Nishimura and Hata (Osaka University, Japan). Digoxigenin-labeled antisense and sense probes of *Collagen type II alpha 1 chain* (*Col2a1*), *Collagen type X alpha 1 chain (Col10a1)*, *Aggrecan (Acan)*, *Matrix metalloproteinase 13 (Mmp13)*, *Indian hedghog (Ihh)*, and *Pannexin 3 (Panx3)* were transcribed according to the manufacturer's protocol (Roche, Mannheim, Germany). Sense probes for the negative control did not yield significant staining (data not shown).

2.9. Chondrocyte pellet culture

Mouse chondrocyte pellet culture was performed as described previously [31]. Briefly, costal cartilage was dissected from P0 mice and digested with 0.1% collagenase in Dulbecco's modified Eagle's medium (DMEM). Collected primary chondrocytes were centrifuged in a 15 ml tube at 300 *g* for 10 min to form a chondrocyte pellet (3.0×105 chondrocytes per pellet), cultured in chondrogenic inductive medium (DMEM/F12, 0.1% Dexamethasone, 50 μM L-ascorbic acid 2-phosphate, 40 μg/mL L-proline, and 1 mM Sodium pyruvate) containing 1% ITS Premix (#354351; Corning, NY, USA) at 37 °C under 5% CO_2. The medium was refreshed every other day. After 7 days, total RNA was isolated from pellets for real-time polymerase chain reaction (PCR) analysis. Some pellets were embedded in paraffin for immunohistochemical analysis.

2.10. Real-time PCR analysis

Total RNA was extracted from tibiae growth plates or primary chondrocytes using an RNeasy mini kit (QIAGEN, Hilden, Germany) according to the manufacturer's protocol. cDNA was synthesized from 2 μg total RNA using SuperScript II Reverse Transcriptase and random primers (Thermo Fisher Scientific). Quantitative RT-PCR was performed using THUNDERBIRD SYBR qPCR Mix (TOYOBO, Osaka, Japan) and the 7300 Real-time PCR system (Applied Biosystems, Foster City, CA, USA) according to the manufacturer's protocol. GAPDH expression was used as an internal control. The primer sequences were as follows: *Col2a1*, 5′-acccccaggtgctaatgg-3′ (forward) and 5′-gaacacctttgggaccatctt-3′ (reverse); *Col10a1*, 5′-gcatctcccagcaccaga-3′ (forward) and 5′-ccatgaaccagggtcaagaa-3′ (reverse); *Sox9*, 5′-gtacccgcatctgcacaac-3′ (forward) and 5′-ctcctccacgaagggtctct-3′ (reverse); *Indian hedgehog (Ihh)*, 5′-tgcattgctctgtcaagtctg-3′ (forward) and 5′-gctccccgttctctaggc-3′ (reverse); *Acan*, 5′-cagctgcccttcacatgtaaa-3′ (forward) and 5′-tggacaaagccctcagtacact-3′ (reverse); *Sp7*, 5′-agagatctgagctgggtagagg-3′(forward) and 5′-aagagagcctggcaagagg-3′(reverse); *Spp1*, 5′-cgatgatgatgacgatggag-3′(forward) and 5′-tggcatcaggatactgttcatc-3′(reverse); *Mmp10*, 5′-gcagcccatgaacttggccact-3′ (forward) and 5′-agggaccggctccatacaggg-3′ (reverse); and *Gapdh*, 5′-aactttggcattgtggaagg-3′ (forward) and 5′-acacattggggtaggaaca-3′(reverse).

2.11. Cell proliferation assay

To label proliferating cells, BrdU dissolved in PBS was intraperitoneally administered to pregnant mice at E18.5 and postnatal mice at P7, P14, and P21 at a concentration of 100 μg/g body weight (n = 3 each genotype). Animals were sacrificed 1 h after injection. The BrdU tracing assay was performed as previously described [32]. P14 mice were injected with BrdU twice after an interval of 6 h and sacrificed 48 h after the first injection. Immunohistochemistry for BrdU was carried out as described elsewhere [32] using an anti-BrdU antibody (dilution 1:100). The sections were counterstained with diluted hematoxylin. A rectangle covering the proliferative zone of the epiphyseal cartilage was set, and the numbers of BrdU-positive cells and total cells were counted within the rectangle. The average of three serial sections was calculated as the BrdU number of each individual.

2.12. Microscopy

Histological sections were digitized with a DP72 camera (Olympus Corp., Tokyo, Japan) mounted on a BX50 microscope (Olympus); fluorescent images were captured using a BZ-9000 microscope (Keyence Japan, Osaka, Japan). Figures were prepared using Adobe Photoshop CS6 software (Adobe Systems, San Jose, CA, USA).

2.13. Statistical analysis

Data were statistically analyzed by Student's *t*-test to compare difference between two groups. In case of more two groups, we used a one-way analysis of variance or two-way analysis of variance followed by the Tukey-Kramer test. The data are expressed as the means ± SD; values of $p < 0.05$ were considered significant.

3. Results

3.1. Activation of the alternative NF-κB pathway in the growth plate

We first examined whether the alternative NF-κB pathway was activated in the epiphyseal cartilage by immunofluorescent staining. Previous works showed that the classical NF-κB pathway was activated in the epiphyseal cartilage during embryonic development [15,19]. The translocation of the phosphorylated NF-κB2 and RelB proteins into the nucleus indicates activation of the alternative NF-κB pathway. Immunofluorescent analysis revealed that both proteins were extensively translocated into the nucleus in most chondrocytes in the periarticular zone of the mouse growth plate at E18.5 (Fig. 1A, B, E–G, N–Q, and X). Although both proteins were less prominently translocated into the nucleus in the proliferative zone (Fig. 1A, C, H–J, N, R–T, and X), such

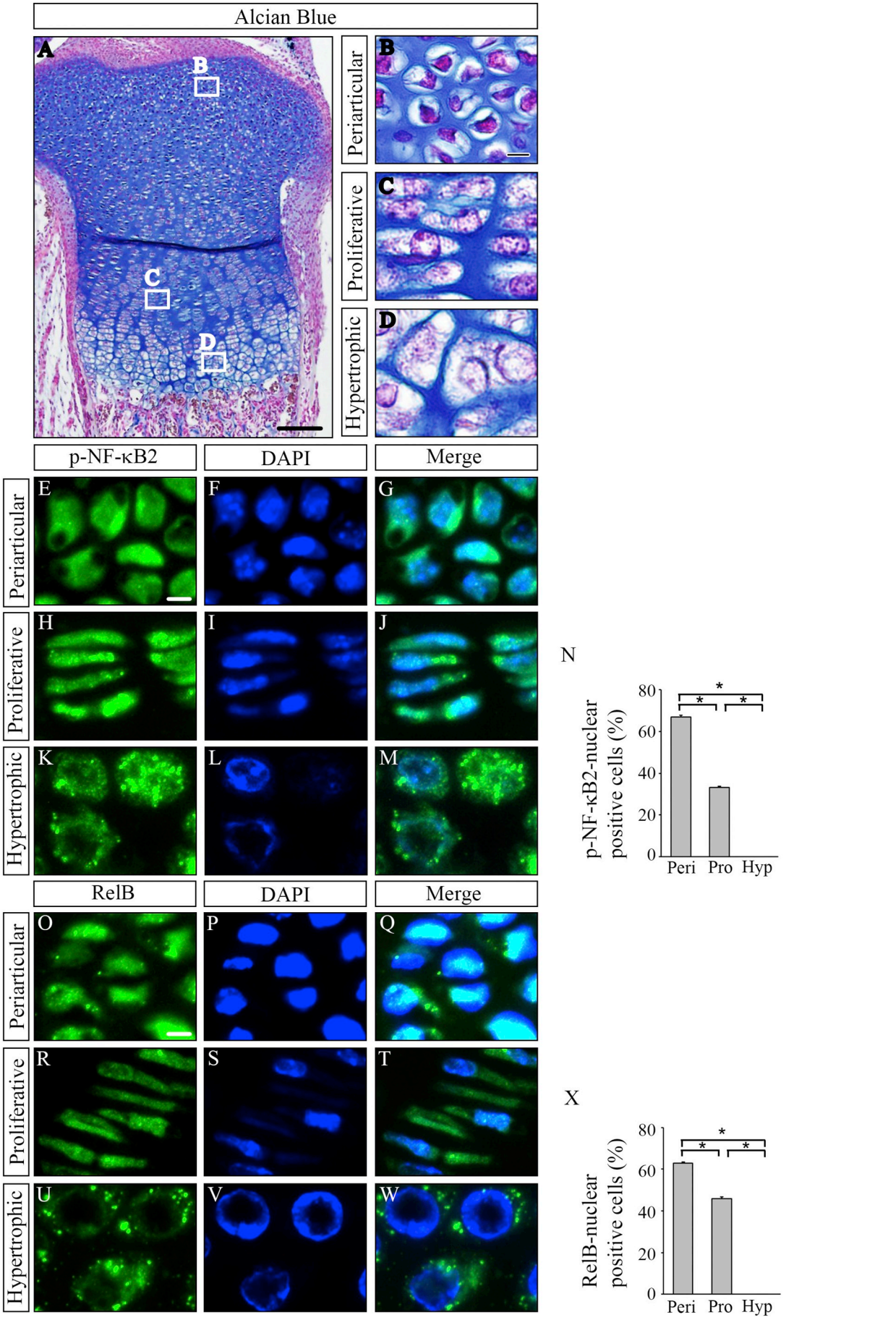

(caption on next page)

Fig. 1. Expression of p-NF-κB2 and RelB in chondrocytes. (A) Alcian Blue staining of the epiphyseal cartilage at postnatal day (P) 0 (n = 4). (B–D) Magnified views of the boxed area in (A). Periarticular (B), proliferative (C), and hypertrophic (D) zones. Immunofluorescence of the p-NF-κB2 (E, H, K) and RelB (O, R, U) proteins in the periarticular (E–G, O–Q), proliferative (H–J, R–T), and hypertrophic (K–M, U–W) zones. The images are representative of three independent experiments. Bars: 100 μm in (A), 10 μm in (B) for (B–D), 10 μm in (E) for (E–M), and 10 μm in (O) for (O–W). Quantitative analyses of ratio of p-NF-κB2 (N) and RelB (X), which translocated into the nucleus in periarticular, proliferative, and hypertrophic zone. Data are presented as the ratio of nuclear translocated cells/total number of chondrocytes/field as the mean ± SD (n = 4). ** $p < 0.01$. (For interpretation of the references to color in this figure legend, the reader is referred to the web version of this article.)

translocation was rarely observed in the hypertrophic zone (Fig. 1A,D, K–N, U–X). No signal was detected using control IgG (Fig. S1). These results suggest that the alternative NF-κB pathway is activated mainly in the periarticular zone of the growth plate.

3.2. The alternative NF-κB pathway is constitutively activated in *p100*$^{-/-}$ chondrocytes

p100$^{-/-}$ mice exhibited dwarfism and shortened long bones at P7, P14, and P21 (Fig. 2A and B, data not shown). Ossification was less mature in cranial sutures at P7 and the patella at P21 in *p100*$^{-/-}$ mice (Fig. 2C–F). Examination of axial skeleton revealed that the length of each vertebral body of *p100*$^{-/-}$ was shorter than that of WT at P7, P14, and P21 (Fig. S2). It has been reported that the DNA-binding activity of the RelB/p52 complex to the κB site is constitutively activated in lymphoid or nonlymphoid tissues in *p100*$^{-/-}$ mice [27,33,34]. Thus, we hypothesized that the alternative NF-κB pathway is also constitutively activated in chondrocytes in *p100*$^{-/-}$ mice, which would be responsible for the growth disorder of long bones. To test this hypothesis, we analyzed the intracellular localization of the NF-κB2 and RelB proteins in chondrocytes (Fig. 2G–S). Western blot analysis revealed that the amount of NF-κB2 and RelB proteins translocated into the nucleus increased in *p100*$^{-/-}$ chondrocytes obtained from rib cartilage at P0 (Fig. 2G). Immunohistochemistry confirmed that *in vivo*, the NF-κB2 or RelB protein was more intensely translocated into the nucleus in the proliferative zone of the growth plate in *p100*$^{-/-}$ mice than in WT mice at E18.5 (Fig. 2I, L, O and R); the NF-κB2 or RelB protein was translocated into the nucleus at a similar level between WT and *p100*$^{-/-}$ mice in the periarticular zone, and almost no translocation was observed in both genotypes in the hypertrophic zone (Fig. 2H, J, K, M, N, P, Q and S). These results indicate that the alternative NF-κB pathway was indeed constitutively activated in the proliferative chondrocytes in *p100*$^{-/-}$ mice.

3.3. Growth plate abnormalities in *p100*$^{-/-}$ mice

To explore the morphological phenotypes of *p100*$^{-/-}$ mice, time course changes of long bones were histologically analyzed (Fig. 3). The width of the entire growth plate in *p100*$^{-/-}$ mice was narrower than that in WT mice at P21. Moreover, the arrangement of chondrocyte columns in the growth plate was aberrated, and the hypertrophic zone became narrower in *p100*$^{-/-}$ mice (Fig. 3B and E). In the head of the fibula of *p100*$^{-/-}$ mice, hypertrophy of chondrocytes did not sufficiently occur (Fig. 3C and F). A previous study reported that the overall body size of *p100*$^{-/-}$ mice becomes obviously smaller than that of WT mice from P10 to P14 [27]. Although there was no significant difference in the growth plate between WT and *p100*$^{-/-}$ mice at P0 and P7 (Fig. 3G, H, K, L, O, P, S, and T), malformation of the growth plate became prominent from P14 to P21 (Fig. 3I, J, M, N, Q, R, U, and V), suggesting that the effect of the alternative NF-κB pathway being constitutively activated in chondrocytes appears as a phenotype from P14 afterwards.

3.4. The expression of chondrocyte differentiation markers in *p100*$^{-/-}$ mice

Next, the expression patterns of differentiation markers for chondrocytes were examined in tibiae in WT and *p100*$^{-/-}$ mice from P0 to P21 (Fig. 4). *Acan* and *Col2a1* are expressed in resting and proliferating chondrocytes in WT mice, while *Col10a1* and *Mmp13* are expressed in hypertrophic chondrocytes and terminal hypertrophic chondrocytes, respectively [35]. The expression patterns of these markers in *p100*$^{-/-}$ mice were almost identical to those in WT mice at P0, P7, and P14 (Fig. 4A1–3, B1–3, C1–3, D1–3, E1–3, F1–3, G1–3, and H1–3). However, notably, the width of the *Acan*- and *Col2a1*-positive areas was narrower in *p100*$^{-/-}$ mice than in WT mice at P21 (Fig. 4A4–45, B4–5, C4–5, and D4–5). Moreover, the expression of *Col10a1* and *Mmp13* was almost diminished in *p100*$^{-/-}$ mice at P21 (Figs. 4E4–5, F4–5, G4–5, and H4–5, S3). To exclude the possibility that abnormal differentiation of *p100*$^{-/-}$ chondrocytes observed *in vivo* was caused by systematic factors such as nutrition and hormones, chondrocyte pellets derived from WT and *p100*$^{-/-}$ mice were induced to differentiate *ex vivo* (Fig. S4). The size of the *p100*$^{-/-}$ pellets was almost identical to that of the WT pellets (Fig. S4A and B). Expression of the Col II protein was identified in both WT and *p100*$^{-/-}$ pellets (Fig. S4C and D). However, the Col X protein was detected only in WT pellets (Fig. S4E and F). The expression of several chondrogenic marker genes was downregulated in *p100*$^{-/-}$ pellets (Fig. S4G and H). These data suggested that chondrocytes could be relatively normally differentiated in the early phase of chondrogenesis, but the influence of the constitutive activation of the NF-κB pathway appeared in chondrocytes in later stages.

3.5. The decreased proliferative activity in chondrocytes of *p100*$^{-/-}$ mice

To analyze cell proliferative activity in chondrocytes, WT and *p100*$^{-/-}$ mice from E18.5 to P21 were labeled with BrdU for 1 h. Compared with WT mice, the number of BrdU-positive cells in the proliferative area of the growth plate was significantly higher at E18.5 and lower at P7, P14, and P21 in *p100*$^{-/-}$ mice (Fig. 5A–I). Next, an *in vivo* BrdU tracing assay was performed at P14 to clarify whether the decreased number of proliferating chondrocytes in *p100*$^{-/-}$ mice affects the number of chondrocytes in the hypertrophic zone (Fig. 5J and K). In WT mice, a great deal of chondrocytes in the hypertrophic zone were BrdU positive, indicating that the cells, which had undergone proliferation and incorporated BrdU in the proliferative zone, subsequently differentiated. By contrast, few BrdU-labeled cells were observed in both the proliferative and hypertrophic zones in *p100*$^{-/-}$ mice. The reduced number of labeled chondrocytes in the hypertrophic zone was most likely due to less proliferative activity in *p100*$^{-/-}$ mice. These results suggested that proliferative deficiency of chondrocytes in the growth plate of *p100*$^{-/-}$ mice affected proper formation of the hypertrophic zone.

3.6. Unaltered apoptotic activity in chondrocytes of *p100*$^{-/-}$ mice

To analyze the apoptotic activity of chondrocytes, TUNEL staining was performed using WT and *p100*$^{-/-}$ samples from P0 to P21 (Fig. S5). The number of TUNEL-positive cells was not significantly different between WT and *p100*$^{-/-}$ mice in all examined stages.

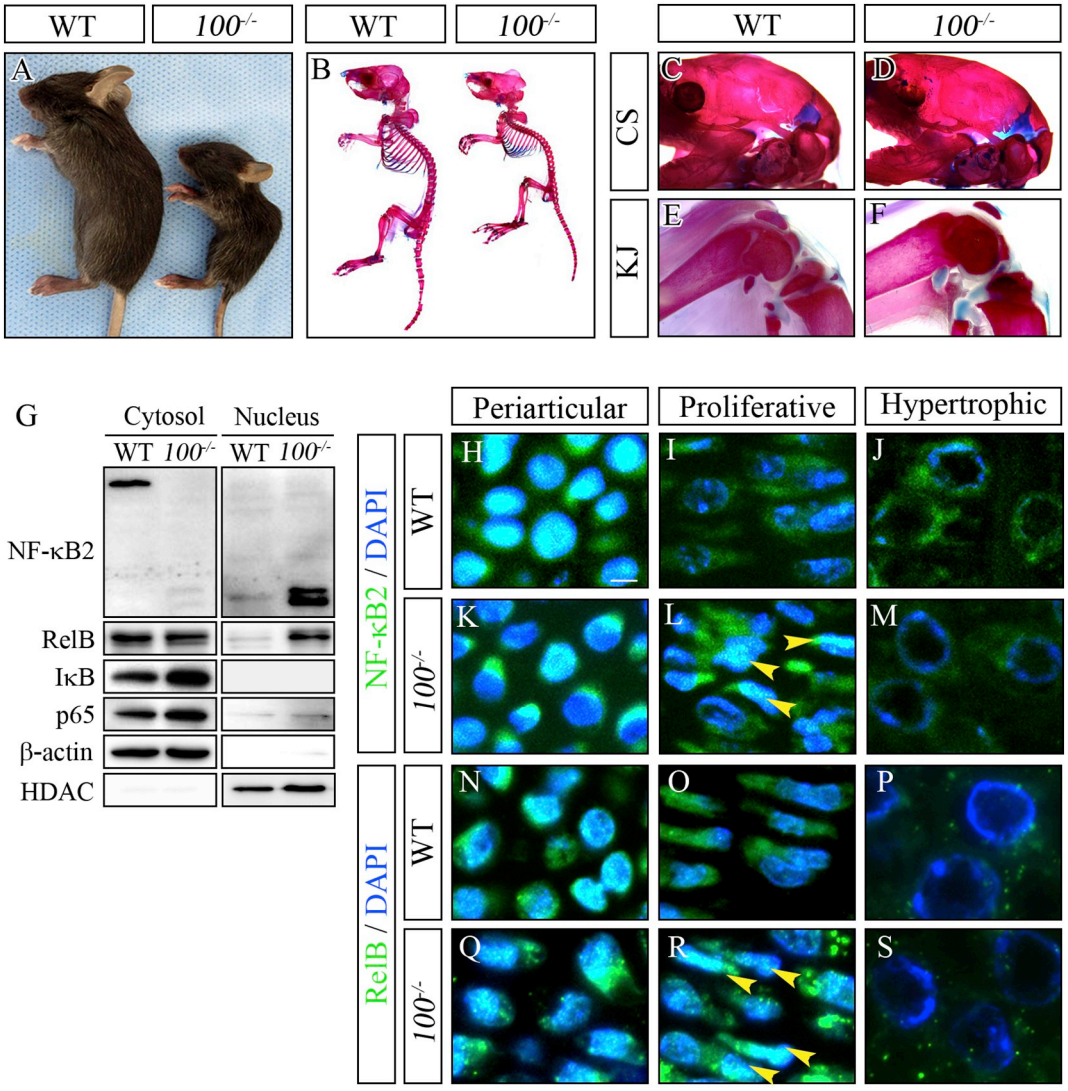

Fig. 2. Comparison of the whole body of WT and *p100*$^{-/-}$ mice and the localization of the NF-κB family proteins in chondrocytes. (A) Whole body view of WT and *p100*$^{-/-}$ mice at P21 (n = 3/each group). (B) Skeletal staining of WT and *p100*$^{-/-}$ mice at P21. (C–F) Ossification of cranial sutures (CS) of WT and *p100*$^{-/-}$ mice at P7 and knee joint (KJ) of WT and *p100*$^{-/-}$ mice at P21 (n = 3/each group). (G) Western blot analysis to detect the localization of NF-κB family proteins in the chondrocytes of WT and *p100*$^{-/-}$ mice at P0. Anti-β-actin and anti-histone deacetylase 1 (HDAC1) were used as a loading control for the cytosol and nuclear extracts, respectively. (H–S) Immunofluorescence of the NF-κB2 (H-M) or RelB (N–S) protein in WT and *p100*$^{-/-}$ mice in the periarticular (H, K, N, Q), proliferative (I, L, Q, R), and hypertrophic (J, M, P, S) zones at P0. The images are representative of three independent experiments. Bar: 10 μm in (H) for (H–S).

3.7. The defect of the growth plate chondrocytes was rescued in p100$^{-/-}$*;RelB*$^{-/-}$ *mice*

It has been demonstrated that the loss of RelB function in *p100*$^{-/-}$ mice can partially rescue developmental defects of B-cell and bone formation by mitigating constitutive activation of the alternative NF-κB pathway [23,34,35]. To test the hypothesis that the deletion of the *RelB* gene can partially rescue the abnormalities observed in the growth plate of *p100*$^{-/-}$ mice, we analyzed *p100*$^{-/-}$*;RelB*$^{-/-}$ mice (Fig. 6). Body size was restored in *p100*$^{-/-}$*;RelB*$^{-/-}$ mice, but it was still smaller than that of WT mice (Fig. 6A). The width of the growth plate of *p100*$^{-/-}$*;RelB*$^{-/-}$ mice was wider than that of *p100*$^{-/-}$ mice to almost a similar level observed in *RelB*$^{-/-}$ mice (Fig. 6B–E). Moreover, the expression patterns of chondrogenic marker genes, such as *Acan*, *Col2a1*, *Col10a1*, and *Mmp13*, were also recovered to a similar level as found in *RelB*$^{-/-}$ mice (Fig. 6F–U). To further analyze whether this restoration was achieved by recovering the proliferation activity of chondrocytes, a BrdU incorporation experiment was performed. Supporting our notion, the number of BrdU-labeled chondrocytes increased in *p100*$^{-/-}$*;RelB*$^{-/-}$ mice compared with *p100*$^{-/-}$ mice (Fig. 6V–Z), suggesting that enhanced activation of p52/RelB binding activity in *p100*$^{-/-}$ mice may cause proliferative defects in chondrocytes, followed by the malformation of the growth plate.

Severe gastric abnormalities, such as a small stomach associated with hyperplasia of the epithelial cell layer, cause premature death in *p100*$^{-/-}$ mice [27]. To clarify whether growth plate defects and subsequent growth disorders, which we observed in *p100*$^{-/-}$ mice, were due to malnutrition, we analyzed gastric phenotypes. Although gastric abnormalities were recognized in both *p100*$^{-/-}$ and *p100*$^{-/-}$*;RelB*$^{-/-}$ mice, the growth plate was restored in *p100*$^{-/-}$*;RelB*$^{-/-}$ mice compared with *p100*$^{-/-}$ mice (Fig. S6). These results indicate that malnutrition may not be the main cause of growth plate disorders of *p100*$^{-/-}$ mice. Rather, these disorders were likely caused by intrinsic chondrocyte abnormalities in *p100*$^{-/-}$ mice.

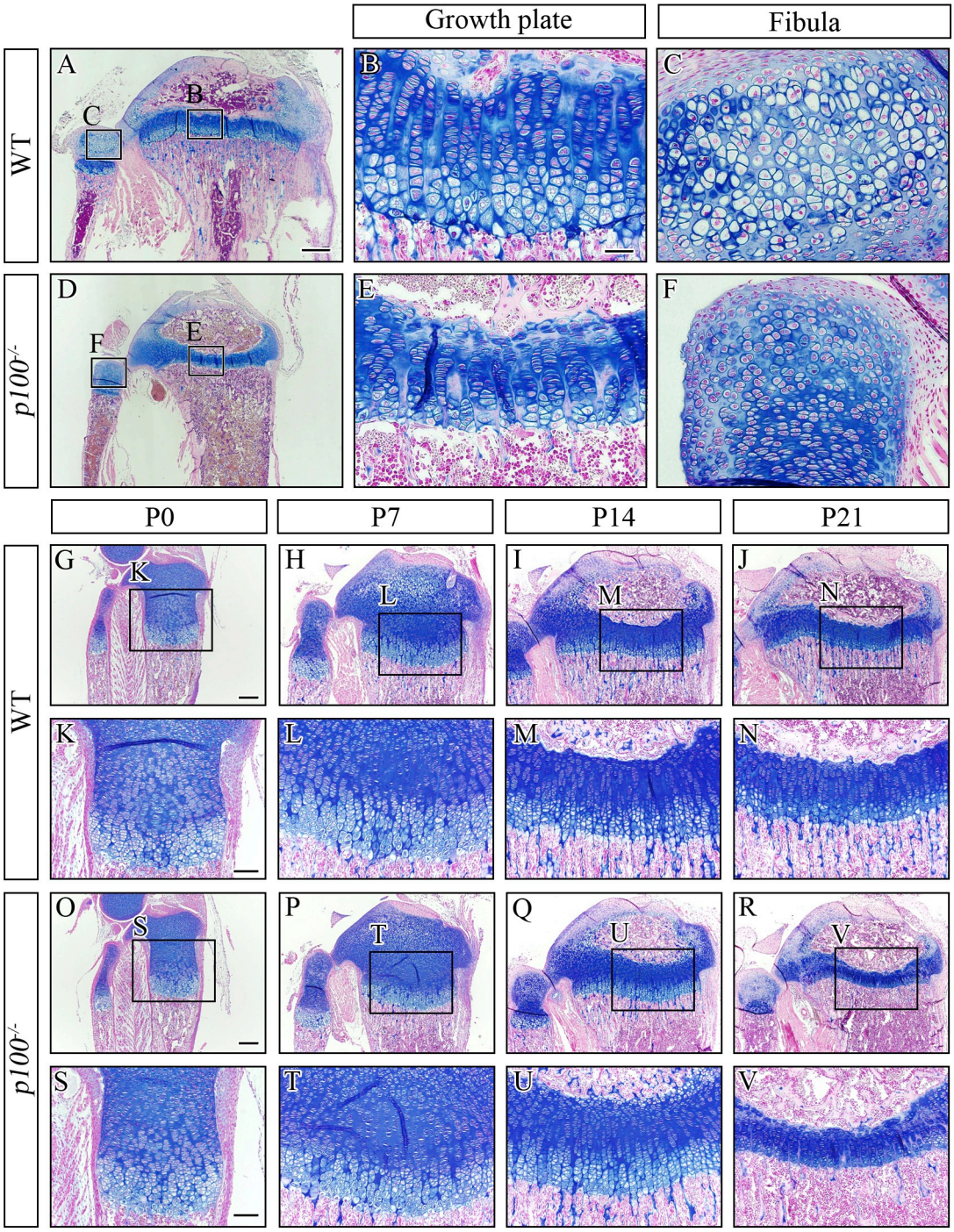

Fig. 3. Histological analysis of the growth plate of WT and $p100^{-/-}$ mice. (A-F) Alcian Blue staining of the epiphysis of the tibiae and the head of fibula at postnatal day (P) 21 (n = 11/each group). (B, C, E, F) Magnified views of the boxed area in growth plate (B, E) and fibula (C, F). (G–V) Chronological phenotypes of the growth plate in WT (G–N) and $p100^{-/-}$ mice (O–V) at P0 (n = 6/each group), P7 (n = 6/each), P14 (n = 6/each group), and P21 (n = 11/each group). The images are representative of at least six independent experiments. Bars: 200 μm in (A) for (A, D), 50 μm in (B) for (B, C, E, F), 200 μm in (G) for (G–J), 100 μm in (K) for (K–N), 200 μm in (O) for (O–R), and 100 μm in (S) for (S–V). (For interpretation of the references to color in this figure legend, the reader is referred to the web version of this article.)

3.8. The expression level of Indian hedgehog (Ihh) or Pannexin 3 (Panx3) correlates with phenotypes of $p100^{-/-}$ and $p100^{-/-}$;$RelB^{-/-}$ mice

Ihh, a member of the hedgehog family, expressed in pre-hypertrophic and hypertrophic chondrocytes and plays critical roles in endochondoral ossification by regulating gene expressions such as parathyroid hormone-related proteins (PTHrP), patched homologue (Ptch1), and ColX [36–39]. Ihh-deficient mice revealed skeletal defects with reduced chondrocyte proliferation and differentiation [38].

Panx3, a member of the pannexins, chordate channel proteins, is also expressed in prehypertrophic and hypertrophic chondrocytes [40–43], suggesting that Panx3 function is required for the transition from proliferation to differentiation in chodrocytes [40,41]. Although proliferative chondrocyte layer in $Panx3^{-/-}$ mice was similar with that of WT mice, hypertrophic and terminal chondrocyte layers were disorganized and much narrow compared with those of WT mice [42,43].

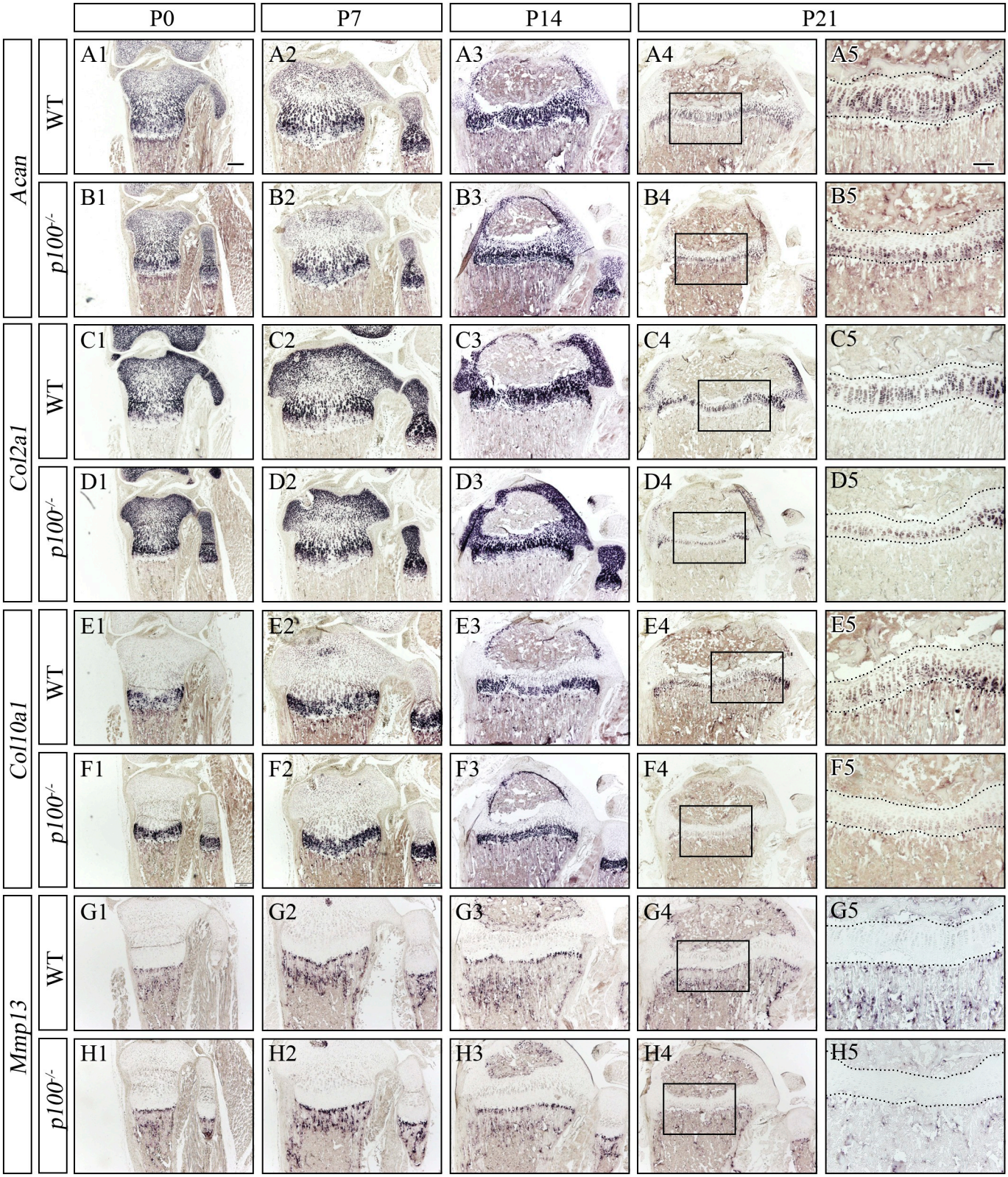

Fig. 4. The expression patterns of differentiation markers for chondrocytes, *Acan* (A1–B5), *Col2a1* (C1–D5), *Col10a1* (E1–F5), and *Mmp13* (G1–H5) in WT and $p100^{-/-}$ mice by section *in situ* hybridization at P0 (n = 3/each group), P7 (n = 4/each), P14 (n = 3/each group), and P21 (n = 7/each group). The images are representative of at least three independent experiments. Bars: 200 μm in (A1) for (A1–4, B1–4, C1–4, D1–4, E1–4, F1–4, G1–4, H1–4) and 100 μm in (A5) for (A5, B5, C5, D5, E5, F5, G5, H5).

These results indicate that Panx3 plays a critical role for maturation of chodrocytes. Thus, we finally examined the expression levels of Ihh and Panx3 in WT, $p100^{-/-}$, and $p100^{-/-}$;$RelB^{-/-}$ mice. Ihh and Panx3 were expressed in both prehypertrophic and hypertrophic chondrocytes in WT mice, while the expression was suppressed in $p100^{-/-}$ mice (Fig. 7A–C, E–G). The expression of Ihh and Panx3 was recovered in

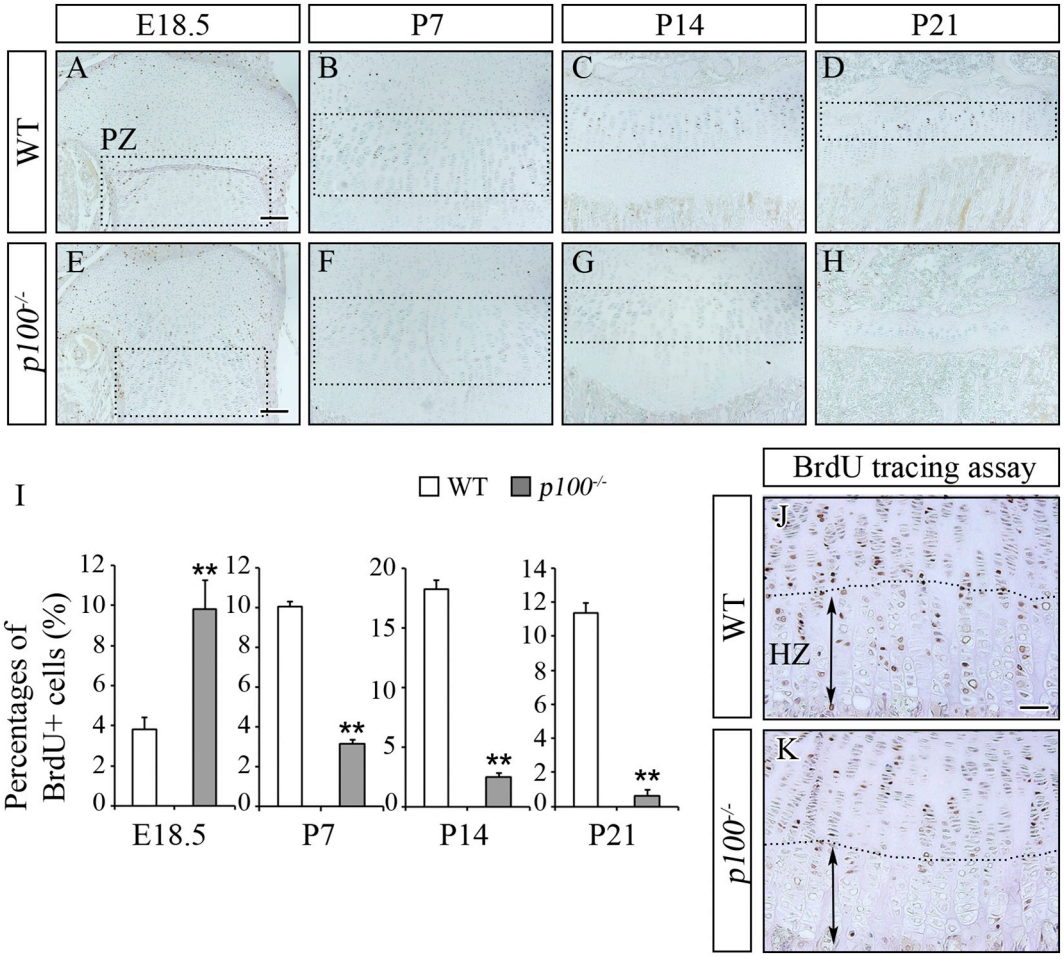

Fig. 5. Proliferative activity of proliferative chondrocytes from E18.5 to P21 in WT and $p100^{-/-}$ mice. (A–H) Squares show BrdU-positive cells in the proliferative zone (PZ) of the growth plate at E18.5 to P21 in WT and $p100^{-/-}$ mice. (I) Quantitative analyses of BrdU-positive cells. BrdU-positive cells were counted and expressed as the number of BrdU-positive cells in five randomly selected fields for each specimen. Data are presented as the percentage of BrdU-positive cells/total number of chondrocytes/field as the mean ± SD (n = 3). ** $p < 0.01$. (J, K) BrdU tracing assay at P14 in WT and $p100^{-/-}$ mice. Double-headed arrows indicate the hypertrophic zone (HZ). The images are representative of three independent experiments. Bars: 100 μm in (A) for (A–D), 100 μm in (E) for (E–H), and 50 μm in (J) for (J, K).

$p100^{-/-}$;$RelB^{-/-}$ mice with similar level of WT mice (Fig. 7D, H).

4. Discussion

It has been reported that the NF-κB signaling pathway, especially the classical NF-κB pathway, is involved in the regulation of chondrocyte differentiation [12–20]. However, little is known regarding the role of the alternative NF-κB pathway in the regulation of chondrocyte differentiation. In the present study, we analyzed chondrocytes of $p100^{-/-}$ mice, in which the alternative NF-κB pathway is constitutively activated, to reveal how the alternative NF-κB pathway is involved in chondrocyte differentiation. Since $p100^{-/-}$ mice exhibited dwarfism, chondrocyte disorder was thought to be one of the causes of this growth abnormality. The growth plate of $p100^{-/-}$ mice was narrower than that of WT mice, and the expression of chondrocyte differentiation marker genes was decreased in $p100^{-/-}$ mice. In addition, proliferative activity was reduced in $p100^{-/-}$ mice. Furthermore, these defects were partly rescued when the *RelB* gene was deleted in $p100^{-/-}$ mice. These data indicated that the constitutively activated alternative NF-κB pathway suppressed both chondrocyte proliferation and differentiation. Notably, bone formation defects in $p100^{-/-}$ appeared earlier in vertebrae than in long bones, which would result in dwarfism phenotype at P21. It should be elucidated in the future study whether proper regulation of NF-κB pathway is required in earlier stages in vertebral development.

It has been noted that *Nfkb2* transcripts are recognized in the thymus, the epithelial cell layer of the stomach, and other various tissues [27]. However, the specific localization of NF-κB2 in the cartilage has been obscure. To ascertain the activated state of the alternative NF-κB pathway in the cartilage of developing limbs, we performed immunofluorescence to detect the nuclear translocation of the NF-κB2 and RelB proteins. These proteins were translocated into the nucleus of periarticular chondrocytes at E18.5, suggesting that the alternative NF-κB pathway has the potential to keep chondrocytes in the resting state. On the other hand, in $p100^{-/-}$ mice, the NF-κB2 or RelB protein was markedly translocated into the nucleus in the proliferative zone. Based on these results, we hypothesize that the abnormally activated alternative NF-κB pathway affects chondrocyte proliferation in $p100^{-/-}$ mice.

To support this hypothesis, a BrdU labeling assay was performed, and the number of BrdU-positive cells remarkably decreased in $p100^{-/-}$ mice at P7, P14, and P21. In contrast, there were twice as many BrdU-positive cells at E18.5, suggesting that the alternative NF-κB pathway may have a chronologically different role in the regulation of chondrocyte proliferation and is important for embryonic chondrogenesis. In addition, the expression levels of some cyclin family genes, such as *Ccnb1*, *Ccnd1*, *Ccnd2*, and *Cdkn1c*, decreased in the chondrocytes derived from $p100^{-/-}$ mice (data not shown).

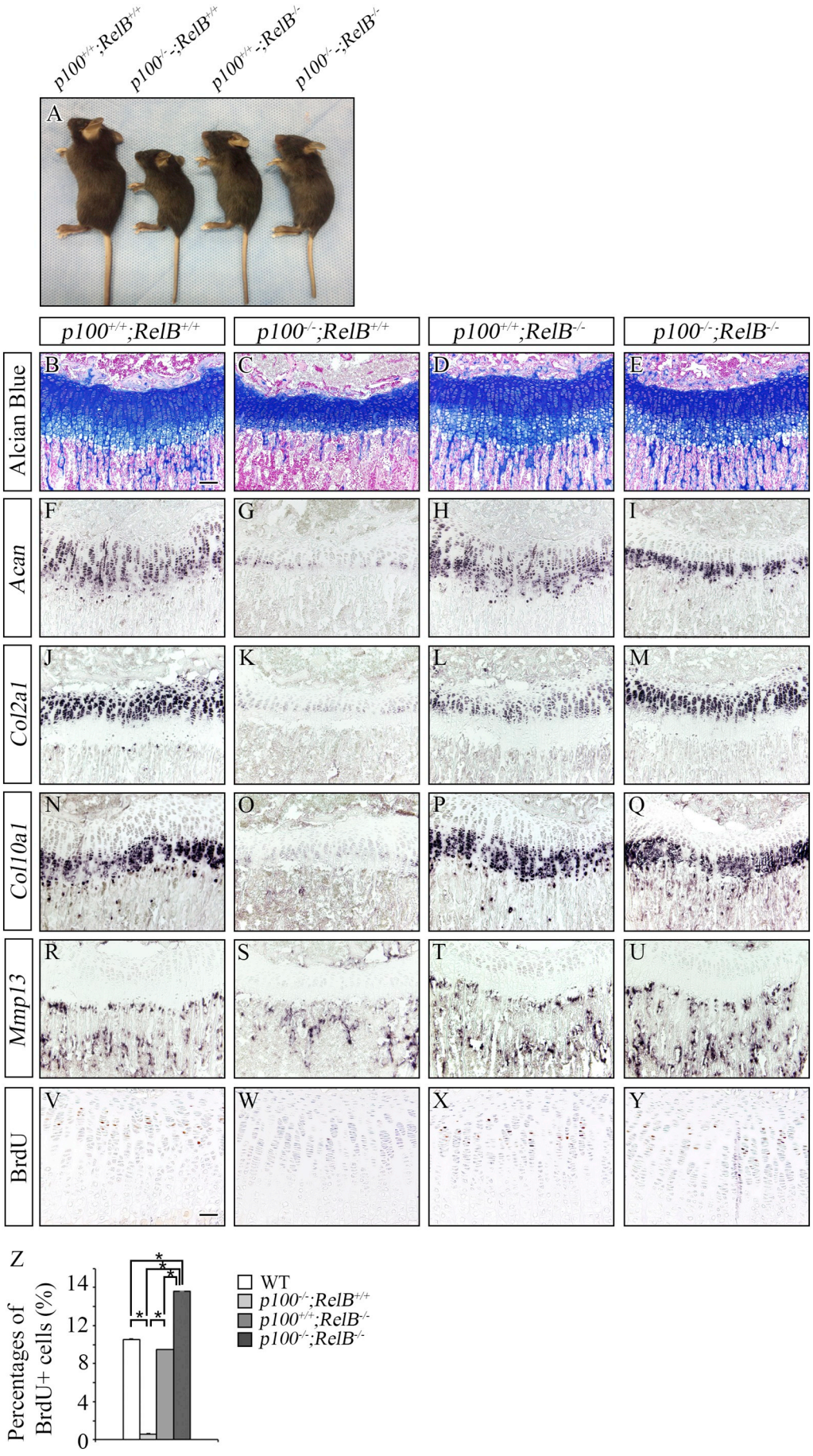

Fig. 6. Endochondral ossification in $p100^{-/-}$ mice is partially rescued by the deletion of RelB. (A) Whole body view of $p100^{+/+};RelB^{+/+}$ (WT), $p100^{-/-};RelB^{+/+}$, $p100^{+/+};RelB^{-/-}$, and $p100^{-/-};RelB^{-/-}$ at P21. (B–E) Morphological analysis of the growth plate of $p100^{+/+};RelB^{+/+}$, $p100^{-/-};RelB^{+/+}$, $p100^{+/+};RelB^{-/-}$, and $p100^{-/-};RelB^{-/-}$ at P21. (F–U) Section *in situ* hybridization of differentiation markers for chondrocytes, *Acan* (F–I), *Col2a1* (J–M), *Col10a1* (N–Q), and *Mmp13* (R-U). (V–Y) BrdU incorporation experiment in the growth plate of $p100^{+/+};RelB^{+/+}$, $p100^{-/-};RelB^{+/+}$, $p100^{+/+};RelB^{-/-}$, and $p100^{-/-};RelB^{-/-}$ at P14. The images are representative of three independent experiments. Bars, 100 μm in (B) for (B–U), 50 μm in (V) for (V–Y). (Z) Quantitative analyses of BrdU-positive cells. BrdU-positive cells were counted and expressed as the number of BrdU-positive cells in five randomly selected fields for each specimen. Data are presented as the percentage of BrdU-positive cells/total number of chondrocytes/field as the mean ± SD (n = 3). * $p < 0.05$.

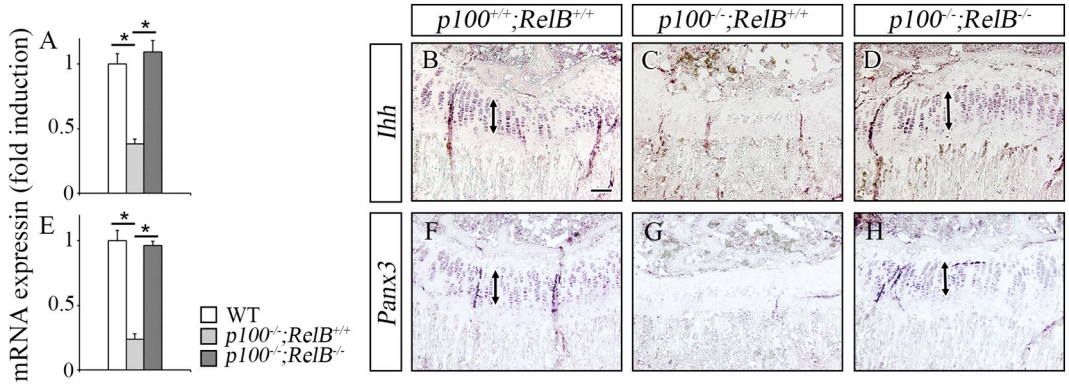

Fig. 7. The expression level of Indian hedgehog (Ihh) or Pannexin3 (Panx3) correlates with phenotypes of $p100^{-/-}$ and $p100^{-/-};RelB^{-/-}$ mice. (A) Quantitative RT-PCR analysis of Ihh mRNA in cartilage of WT, $p100^{-/-}$, and $p100^{-/-};RelB^{-/-}$ mice. Data are expressed as the mean ± SD (n = 3). *p < 0.05. (B-D) *Ihh* in WT (B), $p100^{-/-}$ (C), and $p100^{-/-};RelB^{-/-}$ (D) mice by section *in situ* hybridization. The images are representative of three independent experiments. (E) Quantitative RT-PCR analysis of Panx3 mRNA in cartilage of WT, $p100^{-/-}$, and $p100^{-/-};RelB^{-/-}$ mice. Data are expressed as the mean ± SD (n = 3). *p < 0.05. (F–H) *Panx3* in WT (F), $p100^{-/-}$ (G), and $p100^{-/-};RelB^{-/-}$ (H) mice by section *in situ* hybridization. The images are representative of three independent experiments. Bar: 200 μm.

Furthermore, the BrdU tracing assay indicated that decreased proliferative activity caused deprivation of the source cells, which can differentiate into hypertrophic chondrocytes in $p100^{-/-}$ mice. As constitutive activation of the alternative NF-κB pathway strongly stimulated cell proliferation in embryos, cell source would be depleted during normal chondrocyte development after birth. Actually, the expression of chondrocyte differentiation marker genes, such as *Col10a1* and *Mmp13*, decreased in $p100^{-/-}$ mice.

Guo and colleagues have shown that constitutively activated RelB activity caused by p100 deficiency affected normal B-cell development [33,34]. Moreover, disturbed B-cell development in $p100^{-/-}$ mice can be rescued by deletion of one or both alleles of the *RelB* gene [35]. They suggested that proper regulation of the processing of the p100 protein and p52/RelB DNA-binding activity was needed for B-cell development [35]. Another study demonstrated that deletion of one or both alleles of the *RelB* gene can rescue the osteoporotic phenotype of $p100^{-/-}$ mice, although deletion of both *RelB* alleles resulted in enhanced bone formation [27]. According to the above reports, we hypothesized that abrogating RelB activity in $p100^{-/-};RelB^{-/-}$ double mutant mice could partially rescue the chondrocyte abnormalities observed in $p100^{-/-}$ mice. The defect in the width of the $p100^{-/-}$ growth plate was restored in $p100^{-/-};RelB^{-/-}$ mice. Furthermore, the expression levels of chondrocyte differentiation marker genes and proliferative activity were recovered in $p100^{-/-};RelB^{-/-}$ mice. The expression levels of some cyclin family genes, such as *Ccnb1*, *Ccnd2*, and *Cdkn1c*, were recovered in $p100^{-/-};RelB^{-/-}$ mice (data not shown). Our data suggest that proper regulation of the alternative NF-κB pathway is essential for chondrocyte proliferation and differentiation.

Several growth factors, such as bone morphogenetic proteins (BMPs), fibroblast growth factors (FGFs), PTHrP and Ihh are expressed in chondrocytes and locally regulate chondrocyte differentiation [1–3]. Among them, Ihh is expressed in articular chondrocytes at sites of prehypertrophic differentiation. Ihh induces PTHrP expression, which inhibits chondrocyte hypertrophy, and further suppresses Ihh expression by maintaining chondrocytes in a proliferating stage [36–38]. Ihh also plays crucial roles in chondrocyte proliferation and differentiation independent of PTHrP signaling [44,45]. The pannexin family consists of three members, Panx1, Panx2, and Panx3, chordate channel proteins as gap junction proteins [46]. Although Panx3 is expressed in various tissues such as skin, kidney, and spleen, it is highly expressed in skeletal tissues such as cartilage and osteoblasts [40,41]. Panx3 is expressed in prehypertrophic and hypertrophic chondrocytes, and mature osteoblasts, but not in proliferative chondrocytes, suggesting that Panx3 plays a role in hypertrophic chondrocyte and osteoblast differentiation. Supporting this hypothesis, $Panx3^{-/-}$ mice revealed delays in hypertrophic chondrocyte and osteoblast differentiation, resulting in shortened long bones in adults [42,43]. In this study, the expression level of Ihh or Panx3 correlates with phenotypes of WT, $p100^{-/-}$, and $p100^{-/-};RelB^{-/-}$ mice, suggesting that reduced expression of Ihh or Panx3 by constitutively activated alternative NF-κB pathway suppresses chondrocyte proliferation and maturation. However, because decreased proliferation and maturation of chondrocytes were observed after P14, further studies are necessary to examine the temporospatial regulatory mechanism by which constitutively activated alternative NF-κB pathway suppresses Ihh or Panx3 expression.

$p100^{-/-}$ mice have various systemic defects such as gastric hyperplasia, histopathological alterations of hematopoietic tissues, and osteoporosis. Ninety percent of $p100^{-/-}$ mice die within the first four postnatal weeks, and they cannot survive beyond 10 weeks [27]. It has been reported that the main cause of this premature death is gastric abnormalities, such as occluded gastric lumen, which cannot contain sufficient milk and food [27]. There was a possibility that malnutrition and other systemic factors caused the defects in chondrocytes and the growth disorders in $p100^{-/-}$ mice. We performed pellet culture as an *ex vivo* differentiation experiment to exclude this possibility. The expression of the Col X protein and several differentiation marker genes decreased in chondrocyte pellets derived from $p100^{-/-}$ mice. Moreover, we compared the stomachs of $p100^{-/-}$ and $p100^{-/-};RelB^{-/-}$ mice to investigate whether the gastric disorder and the chondrocyte disorder were rescued in $p100^{-/-};RelB^{-/-}$ mice. The gastric abnormalities were recognized not only in $p100^{-/-}$ but also in $p100^{-/-};RelB^{-/-}$ mice. These results suggested that malnutrition was not the main cause of the growth plate disorders in $p100^{-/-}$ mice. Since the proliferating cells were gradually decreasing after birth, growth might be affected soon, but the structure of chondrocyte columns had been already built and it would be affected later. Conditional mutant mice, which have the chondrocyte-specific deletion of the C-terminal region of p100 protein, should be generated to analyze the role of the alternative NF-κB pathway in the regulation of chondrocytes in a more detailed manner.

5. Conclusion

The classical NF-κB activity regulates proliferation, differentiation, and apoptosis in chondrocytes [12–20]. Recent findings indicate that constitutive activation of the classical NF-κB pathway in chondrogenic and osteogenic lineage reflecting inflammatory situation suppressed their differentiation and bone formation *in vivo* [20]. Our study

indicated the possibility that the alternative NF-κB pathway has a novel role in regulating chondrocyte proliferation and differentiation. Further studies will be required to elucidate the molecular mechanism of chondrocyte regulation.

Supplementary data to this article can be found online at https://doi.org/10.1016/j.bone.2019.01.002.

Acknowledgments

We thank Drs. Riko Nishimura and Kenji Hata (Osaka University, Japan) for providing the *Ihh* probe for *in situ* hybridization. This work is dedicated to Professor Falk Weih (1959–2014). This work was supported by grants-in-aid from Kyushu Dental University Internal Grants (to E.J.) and from the Research Fellowship for Young Scientists (JP16J09963 to C.N.).

Authors' contribution

C.N. performed the experiments and prepared the initial version of the paper. C.N. and M.N. prepared the histological samples. T.K. provided probes for *in situ* hybridization. T.D-I., N. I., and F.W. provided the *p100*$^{-/-}$ and *RelB*$^{-/-}$ mice. T.I. provides *pannexin3* (Panx3) cDNA and M.M. prepared the Panx3 probe for *in situ* hybridization. C.N., M.N., T.M., T.K., T.D-I., N.I., T.I., M.M., and S.K. reviewed the intermediate draft. E.J. designed the study, performed the literature review, prepared the final versions of the paper, and submitted the document.

Conflict of interest

The authors have declared no conflicts of interest.

References

[1] H.M. Kronenberg, Developmental regulation of the growth plate, Nature 423 (2003) 332–336.
[2] F. Long, F.D.M. Ornitz, Development of the endochondral skeleton, Cold Spring Harb. Perspect. Biol. 5 (2013) a008334.
[3] K. Hata, Y. Takahata, T. Murakami, R. Nishimura, Transcriptional network controlling endochondral ossification, J. Bone Metab. 24 (2017) 147–153.
[4] J.W. Foster, M.A. Dominguez-Steglich, S. Guioli, C. Kwok, P.A. Weller, M. Stevanović, J. Weissenbach, S. Mansour, I.D. Young, P.N. Goodfellow, J.D. Brook, A.J. Scafer, Campomelic dysplasia and autosomal sex reversal caused by mutations in an SRY-related gene, Nature 372 (1994) 525–530.
[5] T. Wagner, J. Wirth, J. Meyer, B. Zabel, M. Held, J. Zimmer, J. Pasantes, F.D. Bricarelli, J. Keutel, E. Hustert, U. Wolf, N. Tommerup, W. Schempp, G. Scherer, Autosomal sex reversal and campomelic dysplasia are caused by mutations in and around the SRY-related gene SOX9, Cell 79 (1994) 1111–1120.
[6] H. Akiyama, M.C. Chaboissier, J.F. Martin, A. Schedl, B. de Crombrugghe, The transcription factor Sox9 has essential roles in successive steps of the chondrocyte differentiation pathway and is required for expression of Sox5 and Sox6, Genes Dev. 16 (2002) 2813–2828.
[7] S. Takeda, J.P. Bonnamy, M.J. Owen, P. Ducy, G. Karsenty, Continuous expression of Cbfa1 in nonhypertrophic chondrocytes uncovers its ability to induce hypertrophic chondrocyte differentiation and partially rescues Cbfa1-deficient mice, Genes Dev. (2001) 467–481.
[8] M. Inada, T. Yasui, S. Nomura, S. Miyake, K. Deguchi, M. Himeno, M. Sato, H. Yamagiwa, T. Kimura, N. Yasui, T. Ochi, N. Endo, Y. Kitamura, T. Kishimoto, T. Komori, Maturational disturbance of chondrocytes in Cbfa1-deficient mice, Dev. Dyn. 214 (1999) 279–290.
[9] E. Jimi, S. Ghosh, Role of nuclear factor-κB in the immune system and bone, Immunol. Rev. 208 (2005) 80–87.
[10] S. Ghosh, Celebrating 25 years of NF-κB research, Immunol. Rev. 246 (2012) 5–13.
[11] B.R.B. Pires, R.C.M.C. Silva, G.M. Ferreira, E. Abdelhay, NF-κB: two sides of the same coin, Genes (Basel) 9 (2018), https://doi.org/10.3390/genes9010024 pii: E24.
[12] Y. Kanegae, A.T. Tavares, J.C. Izpisúa Belmonte, I.M. Verma, Role of Rel/NF-κB transcription factors during the outgrowth of the vertebrate limb, Nature 392 (1998) 611–614.
[13] K. Takeda, O. Takeuchi, T. Tsujimura, S. Itami, O. Adachi, T. Kawai, H. Sanjo, K. Yoshikawa, N. Terada, S. Akira, Limb and skin abnormalities in mice lacking IKKα, Science 284 (1999) 313–316.
[14] Q. Li, Q. Lu, J.Y. Hwang, D. Büscher, K.F. Lee, J.C. Izpisua-Belmonte, I.M. Verma, IKK-1 deficient miceexhibit abnormal development ofskin and skeleton, Genes Dev. 13 (1999) 1322–1328.
[15] S. Wu, J.K. Flint, G. Rezvani, F. De Luca, Nuclear factor-κB p65 facilitates longitudinal bone growth by inducing growth plate chondrocyte proliferation and differentiation and by preventing apoptosis, J. Biol. Chem. 282 (2007) 33698–33706.
[16] S. Wu, D. Fadoju, G. Rezvani, F. De Luca, Stimulatory effects of insulin-like growth factor-I on growth plate chondrogenesis are mediated by nuclear factor-κB p65, J. Biol. Chem. 283 (2008) 34037–34044.
[17] S. Itoh, T. Saito, M. Hirata, M. Ushita, T. Ikeda, J.R. Woodgett, H. Algül, R.M. Schmid, U.I. Chung, H. Kawaguchi, GSK-3α and GSK-3β proteins are involved in early stages of chondrocyte differentiation with functional redundancy through RelA protein phosphorylation, J. Biol. Chem. 287 (2012) 29227–29236.
[18] H. Kobayashi, M. Hirata, T. Saito, S. Itoh, U.I. Chung, H. Kawaguchi, Transcriptional induction of ADAMTS5 protein by nuclear factor-κB (NF-κB) family member RelA/p65 in chondrocytes during osteoarthritis development, J. Biol. Chem. 288 (2013) 28620–28629.
[19] H. Kobayashi, S.H. Chang, D. Mori, S. Itoh, M. Hirata, Y. Hosaka, Y. Taniguchi, K. Okada, Y. Mori, F. Yano, U.I. Chung, H. Akiyama, H. Kawaguchi, S. Tanaka, T. Saito, Biphasic regulation of chindrocytes by Rela through induction of anti-apoptotic and catabolic target genes, Nat. Commun. 7 (2016) 13336.
[20] G. Swarnkar, K. Zhang, G. Mbalaviele, F. Long, Y. Abu-Amer, Constitutive activation of IKK2/NF-κB impairs osteogenesis and skeletal development, PLoS One 9 (2014) e91421.
[21] D.V. Novack, L. Yin, A. Hagen-Stapleton, R.D. Schreiber, D.V. Goeddel, F.P. Ross, S.L. Teitelbaum, SL. The IκB function of NF-κB2 p100 controls stimulated osteoclastogenesis, J. Exp. Med. 198 (2003) 771–781.
[22] S. Vaira, T. Johnson, A.C. Hirbe, M. Alhawagri, I. Anwisye, B. Sammut, J. O'Neal, W. Zou, K.N. Weilbaecher, R. Faccio, D.V. Novack, RelB is the NF-κB subunit downstream of NIK responsible for osteoclast differentiation, Proc. Natl. Acad. Sci. U. S. A. 105 (2008) 3897–3902.
[23] N.S. Soysa, N. Alles, D. Weih, A. Lovas, A.H. Mian, H. Shimokawa, H. Yasuda, F. Weih, E. Jimi, K. Ohya, K. Aoki, K, the pivotal role of the alternative NF-κB pathway in maintenance of basal bone homeostasis and osteoclastogenesis, J. Bone Miner. Res. 25 (2010) 809–818.
[24] T. Maruyama, H. Fukushima, K. Nakao, M. Shin, H. Yasuda, F. Weih, T. Doi, K. Aoki, N. Alles, K. Ohya, R. Hosokawa, E. Jimi, Processing of the NF-κB2 precursor, p100, to p52 is critical for RANKL-induced osteoclast differentiation, J. Bone Miner. Res. 25 (2010) 1058–1067.
[25] Y. Seo, H. Fukushima, T. Maruyama, K. Nakao-Kuroishi, K. Osawa, K. Nagano, K. Aoki, F. Weih, T. Doi, M. Zhang, K. Ohya, T. Katagiri, R. Hosokawa, E. Jimi, Accumulation of p100, a precursor of NF-κB2, enhances osteoblastic differentiation *in vitro* and bone formation *in vivo* in *aly/aly* mice, Mol. Endocrinol. 26 (2011) 414–422.
[26] Z. Yao, Y. Li, X. Yin, Y. Dong, L. Xing, B.F. Boyce, NF-κB RelB negatively regulates osteoblast differentiation and bone formation, J. Bone Miner. Res. 29 (2014) 866–877.
[27] H. Ishikawa, D. Carrasco, E. Claudio, R.P. Ryseck, R. Bravo, Gastric hyperplasia and increased proliferative responses of lymphocytes in mice lacking the COOH-terminal ankyrin domain of NF-κB2, J. Exp. Med. 186 (1997) 999–1014.
[28] M. Guo, J. Shen, J.H. Kwak, B. Choi, M. Lee, S. Hu, X. Zhang, K. Ting, C.B. Soo, R.H. Chiu, Novel role for cyclophilin A in regulation of chondrogenic commitment and endochondral ossification, Mol. Cell. Biol. 35 (2015) 2119–2130.
[29] J.D. Dignam, R.M. Lebovitz, R.G. Roeder, Accurate transcription initiation by RNA polymerase II in a soluble extract from isolated mammalian nuclei, Nucleic Acids Res. 11 (1983) 1475–1489.
[30] C. Nakatomi, M. Nakatomi, K. Saito, H. Harada, H. Ohshima, The enamel knot-like structure is eternally maintained in the apical bud of postnatal mouse incisors, Arch. Oral Biol. 60 (2015) 1122–1130.
[31] Y. Kato, M. Iwamoto, T. Koike, F. Suzuki, Y. Takano, Terminal differentiation and calcification in rabbit chondrocyte cultures grown in centrifuge tubes: regulation by transforming growth factor beta and serum factors, Proc. Natl. Acad. Sci. U. S. A. 85 (1988) 9552–9556.
[32] M. Nakatomi, I. Morita, K. Eto, M.S. Ota, Sonic hedgehog signaling is important in tooth root development, J. Dent. Res. 85 (2006) 427–431.
[33] F. Guo, D. Weih, E. Meier, F. Weih, Constitutive alternative NF-κB signaling promotes marginal zone B-cell development but disrupts the marginal sinus and induces HEV-like structures in the spleen, Blood 110 (2007) 2381–2389.
[34] F. Guo, S. Tänzer, M. Busslinger, F. Weih, Lack of nuclear factor-κB2/p100 causes a RelB-depentent block in early B lymphopoiesis, Blood 112 (2008) 551–559.
[35] D. Stickens, D.J. Behonick, N. Ortega, B. Heyer, B. Hartenstein, Y. Yu, A.J. Fosang, M. Schorpp-Kistner, P. Angel, Z. Werb, Altered endochondral bone development in matrix metalloproteinase 13-deficient mice, Development 131 (2004) 5883–5895.
[36] A. Vortkamp, K. Lee, B. Lanske, G.V. Segre, H.M. Kronenberg, C.J. Tabin, Regulation of rate of cartilage differentiation by Indian hedgehog and PTH-related protein, Science 273 (1996) 613–622.
[37] B. Lanske, A.C. Karaplis, K. Lee, A. Luz, A. Vortkamp, A. Pirro, M. Karperien, L.H. Defize, C. Ho, R.C. Mulligan, A.B. Abou-Samra, H. Jüppner, G.V. Segre, H.M. Kronenberg, PTH/PTHrP receptor in early development and Indian hedgehog-regulated bone growth, Science 273 (1996) 663–666.
[38] B. St-Jacques, M. Hammerschmidt, A.P. McMahon, Indian hedgehog signaling regulates proliferation and differentiation of chondrocytes and is essential for bone formation, Genes Dev. 13 (1999) 2072–2086.
[39] P.W. Ingham, A.P. McMahon, Hedgehog signaling in animal development: paradigms and principles, Genes Dev. 15 (2001) 3059–3087.
[40] T. Iwamoto, T. Nakamura, A. Doyle, M. Ishikawa, S. de Vega, S. Fukumoto, Y. Yamada, Pannexin 3 regulates intracellular ATP/cAMP levels and promotes chondrocyte differentiation, J. Biol. Chem. 285 (2010) 18948–18958.
[41] S.R. Bond, A. Lau, S. Penuela, A.V. Sampaio, T.M. Underhill, D.W. Laird, C.C. Naus,

Pannexin 3 is a novel target for Runx2, expressed by osteoblasts and mature growth plate chondrocytes, J. Bone Miner. Res. 26 (2011) 2911–2922.
[42] S.K. Oh, J.O. Shin, J.I. Baek, J. Lee, J.W. Bae, H. Ankamerddy, M.J. Kim, T.L. Huh, Z.Y. Ryoo, U.K. Kim, J. Bok, K.Y. Lee, Pannexin 3 is required for normal progression of skeletal development in vertebrates, FASEB J. 29 (2015) 4473–4484.
[43] M. Ishikawa, G.L. Williams, T. Ikeuchi, K. Sakai, S. Fukumoto, Y. Yamada, Pannexin 3 and connexin 43 modulate skeletal development through their distinct functions and expression patterns, J. Cell Sci. 129 (2016) 1018–1030.
[44] S.J. Karp, E. Schipani, B. St-Jacques, J. Hunzelman, H. Kronenberg, A.P. McMahon, Indian hedgehog coordinates endochondral bone growth and morphogenesis via parathyroid hormone related-protein-dependent and -independent pathways, Development 127 (2000) 543–548.
[45] U.I. Chung, E. Schipani, A.P. McMahon, H.M. Kronenberg, Indian hedgehog couples chondrogenesis to osteogenesis in endochondral bone development, J. Clin. Invest. 107 (2001) 295–304.
[46] Y. Panchin, I. Kelmanson, M. Matz, K. Lukyanov, N. Usman, S. Lukyanov, A ubiquitous family of putative gap junction molecules, Curr. Biol. 10 (2000) R473–R474.